Adaptive Approximation-Based Control of Hysteretic Unconventional Actuators

L. Riccardi, D. Naso, B. Turchiano, H. Janocha

Abstract—In this paper we develop an algorithm for adaptive control of unconventional actuators based on Prandtl-Ishlinskii models and Lyapunov design. The chosen family of models is general enough to capture the strongly variable shapes of the hysteresis exhibited by some electro-active materials and has an inverse model that can be computed analytically. The approach proposed in this paper adapts the parameters of the model with a learning law based on the minimization of the tracking error, and handles the parameters having a nonlinear influence on the output of the model by means of linearization. An outer position loop is then introduced to compensate the residual compensation error and further improve the tracking performance. The advantages and limitations of the approach are discussed and confirmed by experiments on a mechatronic position actuator based on magnetic shape memory alloys.

I. INTRODUCTION

IN different fields, ranging from bioengineering to aerospace robotics, the ever wide use of smart materials, such as piezoelectrics or magnetostrictive materials as well as magnetic shape memory alloys (MSMA), shows the capabilities of these new technologies to achieve novel standards in accuracy, efficiency and lightness [1]. In all smart-material-based systems, such as positioning systems or vibration dampers, hysteresis is known to produce poor tracking performance or even instability if not properly handled by the controller.

There are several approaches to control hysteretic systems like MSMA-based actuators. Some of them do not explicitly consider a model of the hysteresis, but exploit some properties, such us the *dissipativity* [2], in order to guarantee stability of the loop with robust and/or adaptive control laws [3],[4]. Other approaches instead rely on the identification of a model that is subsequently inverted to perform feedforward compensation [5],[6]. The cases in which the model is identified online lead to the so-called adaptive hysteresis compensation class of methods. Literature offers a wide choice of phenomenological models for hysteresis, such as the Krasnosel'skii-Pokrovskii (KP) (a complete treatment of this model and its adaptive version can be found in [7] and in the references therein) or the Prandtl-Ishlinskii model (PIM) [8], which are suitable for online identification. The last one has the useful property of allowing the analytical computation of an exact inverse model (while for other Preisach-like operators the inversion has to be computed numerically). Therefore, significant research activities have been carried out in recent years on this subject, see for instance [9], [10], [11]. However, a PIM can describe only hysteresis cycles which are symmetric with respect to the zero point, or the so-called *demagnetized state*. This limitation has been overcome in [12] and [8]. In the latter, a parameterized, memoryless piecewise linear and invertible function is placed in cascade with the PIM to obtain a more general modeling structure called *modified PI model* (MPIM). Unfortunately, the gain in terms of generality of the MPIM comes at the cost of increased complexity of the identification or adaptation problem, because the MPIM is not Linear-In-the-Parameter (LIP) as the standard PIM. Reference [13] addresses this issue by using an alternative definition for model error which leads to a LIP identification problem that is suitable to be solved online. The approach relies on the assumptions that 1) the actuator dynamics, if any, can be neglected, and 2) the hysteresis does not present time-varying offsets.

In this work we present a new control approach for unconventional actuators based on adaptive hysteresis compensation with a MPIM that overcomes the need of the two aforementioned assumptions. The overall control loop includes an adaptive MPIM as basic component, while the remaining dynamics of the actuator system are handled with approximation-based techniques and adaptive bounding. Differently from the mentioned references, the adaptation laws for the parameters of both model and controller are designed by means of Lyapunov methods, which give some guarantees about the stability of the closed loop. The control approach is validated experimentally on a MSMA-based actuator [14]. At present, such actuators are affected by an evident hysteretic behavior, whose offset and shape exhibit a strong dependence on the temperature of material [15], [16]. The paper is organized as follows: Section II briefly

L. Riccardi, D. Naso, B. Turchiano are with, Department of Electronics and Electrical Science (DEE) at the Politecnico di Bari, Bari, Italy. (mail: riccardi@deemail.poliba.it).

H. Janocha is with the Laboratory of Process Automation (LPA) at Saarland University, Saarbruecken, Germany. (mail: janocha@lpa.uni-saarland.de)

summarizes the key elements of the MPIM, while Section III discusses the robust adaptive compensation strategy and the adaptation laws. Finally, Section IV describes the MSMA actuator and summarizes the experimental results, and Section V draws the concluding remarks.

II. THE MODIFIED PRANDTL-ISHLINSKII MODEL

This section offers a brief introduction to the MPIM. For the sake of brevity, we will only recall the key elements of the approach, while referring interested readers to [8] for further details. Hereafter variables i and x indicate the input and the output of the hysteretic system Γ, respectively. Our goal is to identify a model of the system, indicated with $\hat{\Gamma}$, compute its inverse $\hat{\Gamma}^{-1}$ and use it for feedforward compensation. The next subsection will focus on the model family used for $\hat{\Gamma}$, while the subsequent one will discuss the adaptation law presented in [13].

A. The modified Prandtl-Ishlinskii hysteresis operator

Essentially, the MPIM is the cascade of a standard PIM and a memory-free, piecewise linear, parameterized scalar function, called threshold-discrete Prandtl-Ishlinskii Superposition Operator (SO for brevity). The PIM describes a complex hysteresis as the weighted superposition of $N+1$ elementary (backlash or play) operators called *hysterons* (each defined by a single threshold parameter), where N is called the *order* of the PIM. In a compact notation, the PIM can be expressed as:

$$v = H[i] = \sum_{j=0}^{N} p_j H_j\left[i; r_j\right] = \underline{p}^T \underline{H}\left[i; \underline{r}\right], \qquad (1)$$

with $\underline{p} = \left(p_0 .. p_j .. p_N\right)^T$ is the vector of weights, $\underline{H}[i] = \left(H_0[i]..H_j[i]..H_N[i]\right)^T$ is the vector of the elementary operators and $\underline{r}$ is the vector of thresholds.

To overcome the approximation limits of the standard PI model, reference [8] proposes to add a piecewise linear scalar function (called *Superposition Operator*, SO) obtained as the weighted sum of the so-called elementary *one-sided dead-zone operators* (DZO) in series with the PIM. The generic *l-th* DZO depends only on its threshold a_l. The output x of the SO is:

$$x = S(v) = \sum_{l=-L}^{L} w_l S_l\left(v; a_l\right) = \underline{w}^T \underline{S}\left(v; \underline{a}\right), \qquad (2)$$

In (2) it is assumed that the elementary operators are organized in a vector $\underline{S}$ so that the thresholds (also organized in a vector $\underline{a}$) form an ordered sequence $a_{-L} < .. < a_0 = 0 < .. < a_L$. As a consequence, the SO has $2L+1$ elementary operators, where L is called the *order* of the SO. To simplify the notation, hereafter we will drop the dependence from the thresholds. Thus, the modified PI model Γ (MPIM) is defined as the series between the PIM and the SO, i.e.,

$$x = \Gamma[i] = \underline{w}^T \underline{S}\left(\underline{p}^T \underline{H}[i]\right). \qquad (3)$$

As discussed in [8], the inverse MPIM Γ^{-1} (IMPIM) can be computed analytically as the series between the Inverse SO (ISO) and the Inverse PI (IPI), i.e.,

$$i = \Gamma^{-1}[x] = \underline{p}_I^T \underline{H}_I\left[\underline{w}_I^T \underline{S}_I(x)\right]. \qquad (4)$$

The inversion obviously requires that both PIM and SO are invertible, a circumstance that occurs if and only if the weights $\underline{p}$ and $\underline{w}$ satisfy some inequality constraints [8] related to monotonicity properties. Note that the IPI and ISO have the same structure of their direct counterparts, but their weights and thresholds are different. There is a unique, direct mapping between the weights and thresholds of the MPIM and the corresponding weights and thresholds of the IMPIM. If the firsts are available, the others can be readily calculated.

Remark 1: the MPIM family does not consider the presence of an offset in the hysteretic output, and therefore, if needed, it has to be added externally, i.e., $x = \Gamma[i] + \sigma$.

B. Adaptive compensation of hysteresis with MPIM

Due to their complex nonlinear influence on the output of the model, related literature ([8], [10]) tends to define all the thresholds of the MPIM (i.e, vectors $\underline{a}$ and $\underline{r}$) a priori, by means of preliminarily available information on input and output signals, and then focuses on the adaptation of weights $\underline{w}$ and $\underline{p}$. This approach is also adopted in this paper.

Reference [13] develops an adaptation strategy for the weights $\underline{w}_I$ and $\underline{p}$ of a MPIM. In order to have a LIP problem, the authors define model error as $e_1 = H[i] - S^{-1}(x)$ and then determine adaptation laws for $\underline{w}_I$ and $\underline{p}$ which minimize its L_2-norm over a time-interval of interest. The approach has the advantage of considering an error metric e_1 that is LIP with respect to both $\underline{w}_I$ and $\underline{p}$, and the disadvantage that minimizing e_1 does not necessarily guarantee that the actual compensation performance is optimized. For instance, in the case that the output has an offset (see *Remark 1*), or in the case that the output of the hysteresis is not directly measurable, the method may provide unsatisfactory results. Note that the method proposed in [13] does not allow considering the presence of further dynamics in the hysteretic actuator. A way to overcome these limitations will be discussed in the next section.

III. ROBUST ADAPTIVE CONTROL DESIGN

A common representation of unconventional actuators is the series of a hysteretic nonlinearity and a linear dynamics that can describe, for example, the behavior of actuated mechanical loads [17]. In this paper, we will adopt this scheme although it may be noticed that the same ideas could

be extended to the case of nonlinear dynamics by means of adaptive feedback linearization [18].
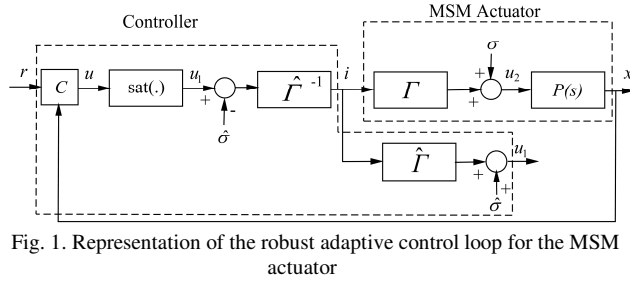
Fig. 1. Representation of the robust adaptive control loop for the MSM actuator

A. Problem statement

For brevity, let us refer to Fig. 1. The MSM actuator is described as the series of a MPIM hysteresis operator Γ with offset σ, and a linear dynamics $P(s)$, where s denotes the Laplace variable. We assume that $P(s)$ can be described by a first-order linear system [16]

$$P(s) = \frac{\lambda^*}{s + \lambda^*}, \qquad (5)$$

where λ^* is an unknown positive constant. Let us assume that the vectors $\underline{p}^*$, $\underline{w}^*$ define the MPIM $\Gamma^* = \Gamma(\underline{p}^*, \underline{w}^*)$ that, together with the offset parameter σ^*, produces the best available approximation of the actual hysteretic phenomenon $\Gamma + \sigma$. Therefore, it can be stated that

$$u_2 = \Gamma[i] + \sigma = \Gamma^*[i] + \sigma^* + \varepsilon_M, \qquad (6)$$

where ε_M defines the minimum functional approximation error (MFAE) which takes into account the ineliminable discrepancies between the chosen class of models and the actual hysteretic phenomenon, as well as any other neglected uncertainty. The current i is the output of the robust adaptive controller, which makes use of an estimated MPIM $\hat{\Gamma} = \Gamma(\hat{\underline{p}}, \hat{\underline{w}})$, an estimated offset $\hat{\sigma}$ and an estimated MPIM compensator $\hat{\Gamma}^{-1}$. The parameters $\hat{\underline{p}}$, $\hat{\underline{w}}$ and $\hat{\sigma}$ represent the estimates of the corresponding best values $\underline{p}^*$, $\underline{w}^*$ and σ^* at the considered time instant.

According to Fig. 1, we can write $u_2 = \Gamma^*[i] + \sigma^* + \varepsilon_M$ and $u_1 = \hat{\Gamma}[i] + \hat{\sigma}$. Thus,

$$u_1 - u_2 = \hat{\Gamma}[i] - \Gamma^*[i] + \hat{\sigma} - \sigma^* - \varepsilon_M, \qquad (7)$$

i.e., the difference between the control action u_1 and the actual output of the hysteresis u_2 depends on the model error.

The overall system in Fig. 1 can be expressed by the following equations:

$$\begin{cases} \dot{x} = -\lambda^* x + \lambda^* u_2 \\ u_2 = u_1 - \left(\tilde{\Gamma} + \tilde{\sigma} - \varepsilon_M \right), \\ u_1 = \mathrm{sat}(u) \end{cases} \qquad (8)$$

where $\tilde{\Gamma} = \hat{\Gamma} - \Gamma^*$, $\tilde{\sigma} = \hat{\sigma} - \sigma^*$, and

$$\mathrm{sat}(u) = \begin{cases} u & \text{if } u_L \leq |u| \leq u_U \\ (u_L \text{ if } u \leq u_L) \text{ or } (u_U \text{ if } u \geq u_U) \end{cases}. \qquad (9)$$

The goal of the robust adaptive controller is to ensure that the output x of the system (8) follows a desired trajectory x_D which is generated by filtering of a reference trajectory r, as follows:

$$\dot{x}_D = -\alpha x_D + \alpha r, \qquad (10)$$

where $\alpha > 0$ is a design constant. In order to take into account the saturation, let us consider the *support variable z* [19]:

$$\dot{z} = -\alpha z + \hat{\lambda}(u_1 - u), \qquad (11)$$

where $\hat{\lambda}$ is an estimate of λ^*. We define the estimation error $\tilde{\lambda} = \hat{\lambda} - \lambda^*$. Variable z describes the contribution of the saturation on the output variable x. If the control variable is within the saturation limits, then $u_1 - u = 0$ and $z \to 0$ in a time interval depending on α. In order to introduce an integral term in the control action, we define the filtered modified tracking error (*filtered error* for brevity) as:

$$e_F = e_M + k \int_0^t e_M \, \mathrm{d}\tau, \qquad (12)$$

where $e_M = (x - x_D - z)$.

We notice that $(x - x_D - z)$ asymptotically converges to the standard tracking error $e_T = x - x_D$ if the control action does not saturate (i.e., if $z = 0$).

Combining (12), (11), (10) and (8) the filtered error dynamics become:

$$\begin{aligned} \dot{e}_F = {} & -\lambda^* x - \tilde{\lambda} u_1 - \lambda^* \left(\tilde{\Gamma} + \tilde{\sigma} - \varepsilon_M \right) \\ & + \alpha(x_D - r + z) + \hat{\lambda} u + k e_M \end{aligned}. \qquad (13)$$

Let us now consider the following control law:

$$u = \frac{1}{\hat{\lambda}} \left(\alpha r + \hat{\lambda} x - k e_M - \alpha x - \alpha k \int_0^t e_M \, \mathrm{d}\tau - \eta(e_F) \right), (14)$$

where $\eta(e_F)$ is a further control term which aims at compensating the various approximation and modeling errors with a strategy that will be defined later on. Using (14), equation (13) can be rewritten as follows:

$$\dot{e}_F = \tilde{\lambda}(x - u_1) - \lambda^* \left(\tilde{\Gamma} + \tilde{\sigma} - \varepsilon_M \right) - \alpha e_F - \eta(e_F). (15)$$

The next subsections are dedicated to the analysis of the model error $(\tilde{\Gamma} + \tilde{\sigma})$, and the design of the adaptation laws, respectively.

B. Analysis of MPIM error

Let us focus on the contribution in (15) due to the hysteresis model error, i.e., $(\tilde{\Gamma} + \tilde{\sigma})$. Some preliminary remarks about the structure of the MPIM may be useful. Since the SO is a weighted sum of activation functions, for any given value of the input signal i, there are a number of activation functions whose output is zero, while other ones provide non-zero contributions that are weighted and summed to build the output. With reference to Fig. 1, even if $\hat{\Gamma}$ and Γ share the same input i, the non-zero activation functions in each system will be different because of the differences between the parameter vectors $\hat{\underline{p}}$ and $\underline{p}^*$ used by the PIM components in the two systems (see (3)).

To illustrate the basic idea, let us analyze the case $\underline{p}^T \underline{H}[i] > 0$. In such a case, only those SO operators whose threshold a_l is smaller than $\underline{p}^T \underline{H}[i]$ will produce a nonzero contribution to the output of the SO. Thus, we can write:

$$\tilde{\Gamma}[i] + \tilde{\sigma} = \sum_{l=0}^{M \leq L} \hat{w}_l \left(\hat{\underline{p}}^T \underline{H}[i] - a_l \right) \\ - \sum_{k=0}^{G \leq L} w_k^* \left(\underline{p}^{*T} \underline{H}[i] - a_k \right) + \tilde{\sigma} \quad , \quad (16)$$

where M is the number of active DZOs in the estimated model at the current time instant, and G is the number of active DZOs in the ideal model. In (16), we used the fact that, when the l-th DZO is active, $S_l(v; a_l) = (v - a_l)$. Clearly, if $\hat{\underline{p}} = \underline{p}^*$, then $M = G$, while in the most general case M and G may be different. In order to perform simplifying operations, we can assume that the output of the ideal model can be written as a weighted sum of the same activated DZOs of the current model plus a further modeling error ε_A taking into account the possible mismatches between M and G. The same reasoning can be applied to the case in which $\underline{p}^T \underline{H}[i] < 0$, and the results can be grouped in matrix notation as follows:

$$\tilde{\Gamma}[i] + \tilde{\sigma} = \\ \hat{\underline{w}}^T \underline{S} \left(\hat{\underline{p}}^T \underline{H}[i] \right) - \underline{w}^{*T} \underline{S} \left(\underline{p}^{*T} \underline{H}[i] \right) + \tilde{\sigma} + \varepsilon_A \quad , \quad (17)$$

where the vector $\underline{S}$ has zero elements for those DZOs which are not active. We can develop the term $\underline{w}^{*T} \underline{S} \left(\underline{p}^{*T} \underline{H}[i] \right)$ with a Taylor series in the point $(\hat{\underline{w}}, \hat{\underline{p}})$, and (17) becomes

$$\tilde{\Gamma}[i] + \tilde{\sigma} = \underline{S}^T \left(\hat{\underline{p}}^T \underline{H}[i] \right) \tilde{\underline{w}} + \hat{\underline{w}}^T \underline{S}_p \tilde{\underline{p}} + \tilde{\sigma} + \varepsilon_1, \quad (18)$$

where $\varepsilon_1 = \varepsilon_A + \varepsilon_T$ and $\underline{S}_p = \partial \underline{S} \left(\hat{\underline{p}}^T \underline{H}[i] \right) / \partial \underline{p}$.

Equations (15), and (18) are in a form that well lends itself to determine adaptation laws using standard Lyapunov design arguments. This step is summarized in the next subsection.

C. Design of the robust adaptive laws

The substitution of (18) into (15) leads to:

$$\dot{e}_F = \tilde{\lambda}(x - u_1) - \alpha e_F - \eta(e_F) + \lambda^* (\varepsilon_M - \varepsilon_1) \\ - \lambda^* \left(\underline{S}^T \left(\hat{\underline{p}}^T \underline{H}[i] \right) \tilde{\underline{w}} + \hat{\underline{w}}^T \underline{S}_p \tilde{\underline{p}} + \tilde{\sigma} \right) \quad (19)$$

We note that the term $(\varepsilon_M - \varepsilon_1)$ represents the overall approximation error, arising from the concurrent presence of the MFAE, activation and linearization errors. Let us define this error as $\varepsilon = \varepsilon_M - \varepsilon_1$. We assume that an unknown upper bound b_U^* and an unknown lower bound b_L^* of ε exist, such that $-b_L^* \leq \lambda^* \varepsilon \leq b_U^*$. Let us introduce the bound estimates $\hat{b}_U$ and $\hat{b}_L$, and the estimation errors $\tilde{b}_U = \hat{b}_U - b_U^*$ and $\tilde{b}_L = \hat{b}_L - b_L^*$. Let us define the control term $\eta(e_F)$ as follows:

$$\eta(e_F) = \begin{cases} -\hat{b}_L & \text{if } e_F < 0 \\ \hat{b}_U & \text{if } e_F \geq 0 \end{cases}, \quad (20)$$

and let us introduce the following adaptive laws

$$\dot{\underline{w}} = \beta \underline{S} \left(\hat{\underline{p}}^T H[i] \right) e_F, \quad (21)$$

$$\dot{\hat{\underline{p}}} = \beta \underline{S}_p^{\,T} \hat{\underline{w}} e_F, \quad (22)$$

$$\dot{\hat{\sigma}} = \beta e_F, \quad (23)$$

$$\dot{\hat{\lambda}} = -\gamma(x - u_1) e_F, \quad (24)$$

$$\dot{\hat{b}}_L = \begin{cases} 0 & \text{if } e_F \geq 0 \\ -\gamma_b e_F & \text{if } e_F < 0 \end{cases}, \quad (25)$$

$$\dot{\hat{b}}_U = \begin{cases} \gamma_b e_F & \text{if } e_F > 0 \\ 0 & \text{if } e_F \leq 0 \end{cases}, \quad (26)$$

where $\beta = \gamma \lambda^* > 0$ is a design constant. Using standard arguments of Lyapunov design theory, it can be proven that the filtered error goes asymptotically to zero and the parameters errors $\tilde{\underline{w}}$, $\tilde{\underline{p}}$, $\tilde{\sigma}$, $\tilde{\lambda}$, $\tilde{b}_L$ and $\tilde{b}_U$ remain uniformly ultimately bounded. However, even though a detailed discussion of these issues goes beyond the space limitations of this paper, it is worth noting that projection of $\dot{\hat{\lambda}}$ is necessary in order to ensure that $\hat{\lambda}$ stays away from zero, and projection of $\dot{\hat{\underline{w}}}$ and $\dot{\hat{\underline{p}}}$ ensures that the resulting MPIM is invertible.

Finally, it can be noted that $\underline{S}_p$ and thus the adaptive law in (22) can be easily computed using the following rules:

$$\frac{\partial S_l(v;a_l)}{\partial \underline{p}} = \begin{cases} \underline{H}[i] & \text{if } v > a_l \text{ and } a_l > 0 \\ \underline{H}[i] & \text{if } v < a_l \text{ and } a_l < 0 \\ \underline{0}^{(N+1)\times 1} & \text{otherwise} \end{cases} \qquad (27)$$

Remark 2: the presented technique uses linearization of the model error by means of Taylor expansion. The approximation is valid if $\|\hat{\underline{p}} - \underline{p}^*\|$ and $\|\hat{\underline{w}} - \underline{w}^*\|$ are small. Thus, our method relies on an off-line identification to start with good estimates of the parameters.

IV. EXPERIMENTAL RESULTS

The main goal of this section is to validate the adaptive approach illustrated before. As an example, we show here the experimental results obtained on a MSMA actuator. First we briefly present the actuator, then the tracking results.

A. The MSM positioning actuator

The MSM actuator [15] is composed by three main parts: the magnetic circuit, made by the excitation coils and the flux guide that provides the magnetic field *H* to the element; the MSM element, that is the coupling between the magnetic part and the mechanical part; the mechanical part, composed by a push rod that provides the interface of the device with the external world. Elongation and contraction are measured on one side of the element that is pre-stressed by a spring to have mechanical strain recovery [14]. The current-displacement characteristic is hysteretic, as shown in Fig. 2 and strongly influenced by temperature (see [15]).

In the next sections we show the tracking results that the application of the adaptive approach illustrated in Fig. 1 has given on the MSM actuator.

B. Off-line identification of the hysteresis

To get the values of the thresholds we carried out an off-line identification procedure of the hysteretic model. The current-displacement characteristic at room temperature of our actuator is shown in Fig. 2. It has been used for off-line identification as in [8] with $N = 5$ and $L = 3$. This can provide us with initial values of $\underline{p}$ and $\underline{w}$. Fig. 2 also reports the identification results.
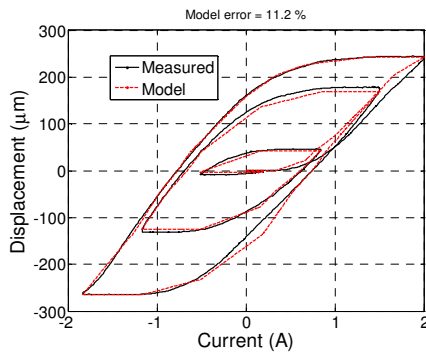
Fig. 2. Hysteresis identified off-line

The percent model error (maximum value of the error divided by the maximum of the output) is 11.2%. The off-line identification offers a static hysteresis compensator that is obviously useless in the case of actuators showing time-varying hysteresis as in our case.

C. Robust adaptive control

We consider two scenarios: in *scenario 1* the tracking of steps is required. Temperature is constant. Fig. 3 shows the tracking result. In the periods where the desired trajectory is constant, the tracking error is within the $\pm 2\mu$m range thanks to the integral action in (12).

In *scenario 2* the tracking of a sum of sinusoids is considered, but this time also applying an external heating/cooling disturbance to the actuator. The experiment is performed as follows. In the first part, the actuators works at room temperature until the time instant $t_1 = 80\,\text{sec}$ evidenced by the first vertical red line in Fig. 4 (bottom). From t_1 the actuator is heated with a heating gun, until $t_2 = 140\,\text{sec}$, where the second vertical red bar is placed in Fig. 4 (bottom). Fig. 4 (top) reports a zoom of the trajectories during the heating. After t_2, the actuator is cooled down with a fan until $t_3 = 200\,\text{sec}$. From Fig. 4 (bottom) it can be observed that the adaptive controller keeps the tracking performance constant. Fig. 5 shows the adaptation of the parameters. The heating process can be recognized in the quick change of all the parameters, with a particularly notable effect on the change of the offset, which coherently with experimental observations increases (decreases) as temperature increases (decreases). The effects of heating can be observed also on the reference current *i* commanded by the controller to the current amplifier (see Fig. 6). When temperature increases, the average of the current shifts to compensate the offset change in the hysteretic behavior. The current saturation values are at ± 2 Amperes. If the heating process is performed for longer time intervals, the current exceeds the saturation limits and the actuator cannot track the desired reference any longer, until the material cools down. Experiments also emphasize that the designer has to choose carefully the reference signal depending on the specific range of operating temperatures for the actuator.

V. CONCLUSION

This paper presents a robust adaptive control strategy for position control of smart-material based actuators. The approach takes into consideration various issues related to such a type of devices, and in particular the presence of a time-varying hysteresis and control action saturation. The hysteresis is addressed by means of an adaptive modified Prandtl-Ishlinskii compensator, whereas the remaining dynamics of the actuator and the saturation are handled with adaptive-approximation based techniques. In order to perform stability analysis, we proposed a novel adaptation strategy for the parameters of the MPIM. The proposed adaptive strategy showed to be effective in various scenarios,

but especially in the case where temperature variations are present and affect the actuator behaviour. The control strategy was in fact able to hold the desired tracking performance.

Future work will consider the extension of the proposed approach to the case of nonlinear dynamics instead of linear ones. Investigations are also in progress to evaluate the benefits of adapting also the thresholds of the MPIM model.

REFERENCES

[1] H. Janocha, *Adaptronics and Smart Structures: basics, materials, design and applications*, Springer, 2007.

[2] R.B. Gorbet, K. a Morris, and D.W.L. Wang, "Passivity-based stability and control of hysteresis in smart actuators," *IEEE Transactions on Control Systems Technology*, vol. 9, 2002, p. 5–16.

[3] B. Jayawardhana, H. Logemann, and E.P. Ryan, "PID control of second-order systems with hysteresis," *International Journal of Control*, vol. 81, 2008, p. 1331.

[4] C.-A. Jiang, M.-C. Deng, and A. Inoue, "Robust stability of nonlinear plants with a non-symmetric Prandtl-Ishlinskii hysteresis model," *International Journal of Automation and Computing*, vol. 7, May. 2010, pp. 213-218.

[5] P. Krejci and K. Kuhnen, "Inverse control of systems with hysteresis and creep," *IEE Proceedings-Control Theory and Applications*, vol. 148, 2001, p. 185–192.

[6] R.V. Iyer, X. Tan, and P.S. Krishnaprasad, "Approximate inversion of the Preisach hysteresis operator with application to control of smart actuators," *IEEE Transactions on Automatic Control*, vol. 50, 2005, pp. 798-810.

[7] R.V. Iyer and X. Tan, "Control of hysteretic systems through inverse compensation," *IEEE Control Systems Magazine*, vol. 29, 2009, p. 83–99.

[8] K. Kuhnen, "Modeling, Identification and Compensation of Complex Hysteretic Nonlinearities: A Modified Prandtl - Ishlinskii Approach," *European Journal of Control*, vol. 9, Aug. 2003, pp. 407-418.

[9] H. Janocha, D. Pesotski, and K. Kuhnen, "FPGA-Based Compensator of Hysteretic Actuator Nonlinearities for Highly Dynamic Applications," *IEEE/ASME Transactions on Mechatronics*, vol. 13, 2008, pp. 112-116.

[10] D. Pesotski, H. Janocha, and K. Kuhnen, "Adaptive Compensation of Hysteretic and Creep Non-linearities in Solid-state Actuators," *Journal of Intelligent Material Systems and Structures*, 2010, vol. 21 no. 14, pp. 1437-1446

[11] Z. Zhang and J.Q. Mao, "Model reference control with adaptive inverse compensation for systems preceded by stress-dependent hysteresis of GMA," *ICCA 2009 -IEEE International Conference on Control and Automation.*, 2009, pp. 673-678.

[12] M. Al Janaideh, Y. Feng, S. Rakheja, Y. Tan, and C.Y. Su, "Generalized Prandtl-Ishlinskii Hysteresis: Modeling and Robust Control for Smart Actuators," *48th IEEE Conference on Decision and Control*, 2009, pp. 7279-7284.

[13] K. Kuhnen and P. Krejci, "Identification of Linear Error-Models with Projected Dynamical Systems," *Mathematical and Computer Modelling of Dynamical Systems*, vol. 10, 2004, p. 59–91.

[14] S. Faehler, "An introduction to actuation mechanisms of Magnetic Shape Memory Alloys," *ECS Transactions*, ECS, 2007, pp. 155-163.

[15] L. Riccardi, G. Ciaccia, D. Naso, B. Turchiano, H. Janocha, "Position Control for a Magnetic Shape Memory Actuator", *IFAC 2010 International Symposium of Mechatronic Systems*, 2010, pp. 478-485

[16] L. Riccardi, D. Naso, B. Turchiano, and H. Janocha, "Robust Adaptive Control of Magnetic Shape Memory Actuators for Precise Positioning," *American Control Conference 2011*, to be published.

[17] J.Y. Gauthier, A. Hubert, and J. Abadie, "Original hybrid control for robotic structures using Magnetic Shape Memory Alloys actuators," *IROS Conference on Intelligent Robots and Systems*, 2007, pp. 747-752.

[18] J.A. Farrell and M.M. Polycarpou, *Adaptive Approximation Based Control*, Wiley InterScience, 2006.

[19] M. Polycarpou, J. Farrell, and M. Sharma, "On-line approximation control of uncertain nonlinear systems: issues with control input saturation," *Proceedings of the 2003 American Control Conference*, 2003, pp. 543-548.
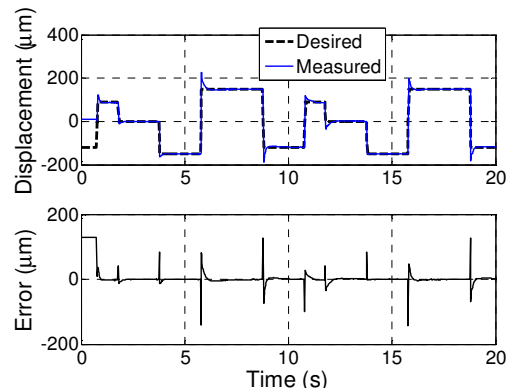
Fig. 3. Tracking of steps
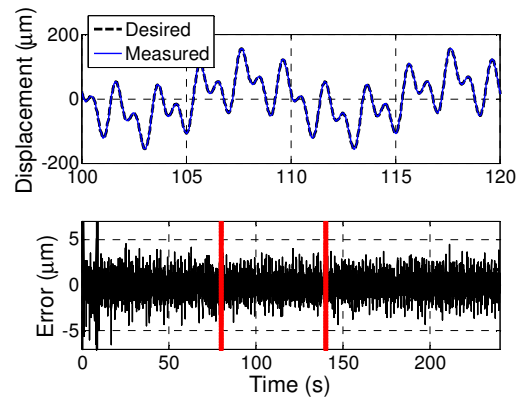
Fig. 4. Tracking of a sum of sinusoids in presence of temperature changes
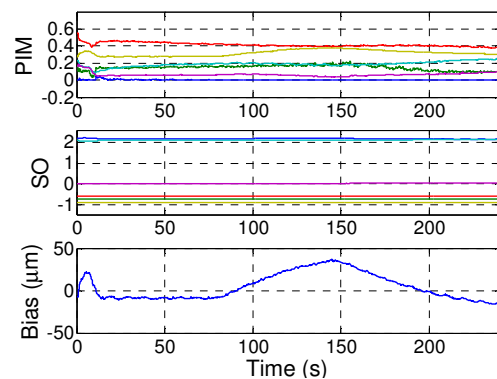
Fig. 5. Adaptation of the parameters during heating/cooling

Fig. 6. Current vs. time